Electronic Supplementary Material (ESI) for Materials Advances.

Supplementary Information

Role of the electronically-active amorphous state in low-temperature processed In_2O_3 thin-film transistors

Ahmad R. Kirmani[1,§], *Emily F. Roe*[1,§], *Christopher M. Stafford*[1], *Lee J. Richter*[1]

[1]Materials Science and Engineering Division, National Institute of Standards and Technology (NIST), Gaithersburg, MD, 20899 USA

[§]Guest Researcher

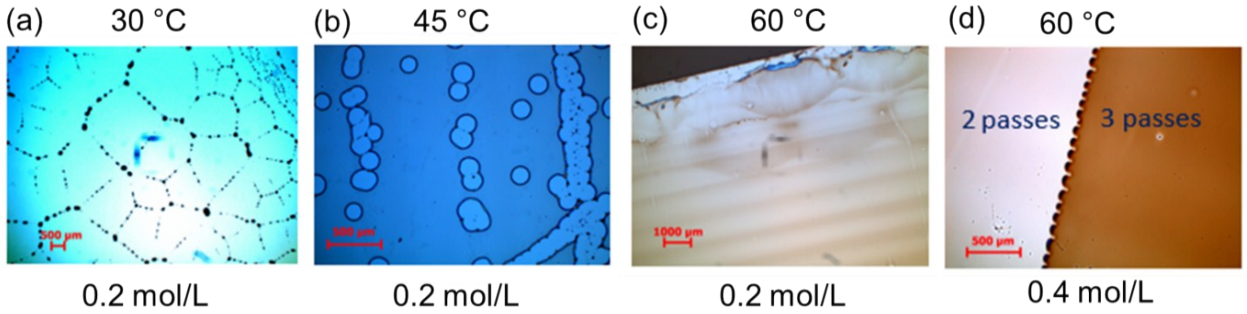

Figure S1. Optical micrographs of sg-In_2O_3 blade-coated films at various substrate temperatures. (d) corresponds to the optimized coating conditions and shows the film after 2 and 3 coats (with 250 °C annealing after each coat).

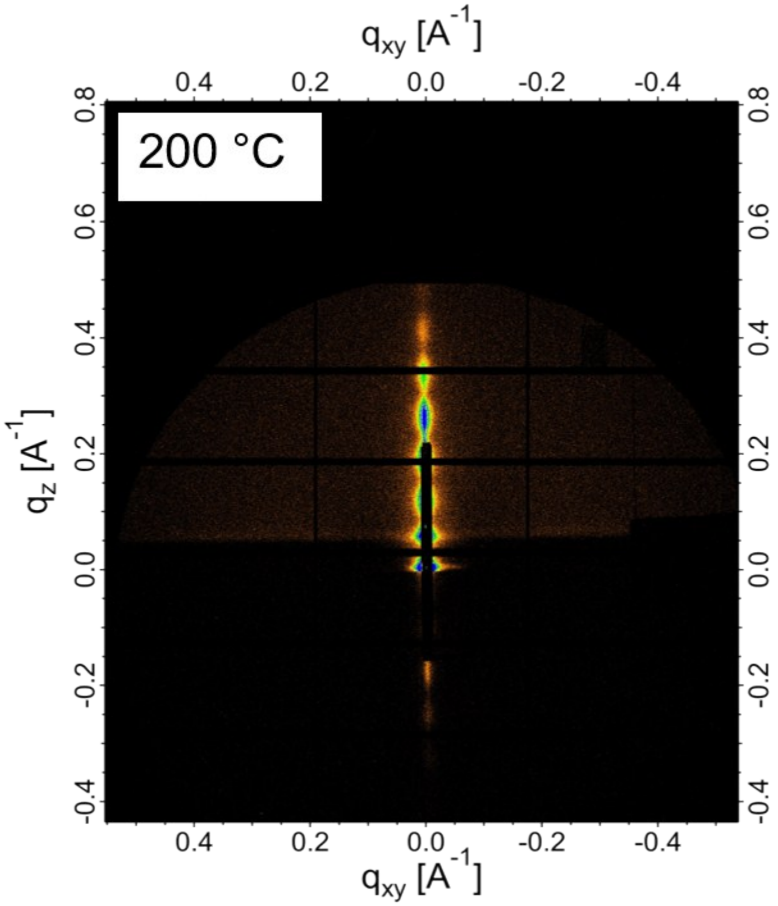

Figure S2. Grazing-incidence small-angle X-ray scattering (GISAXS) pattern of a representative 200 °C annealed bladed sg-In_2O_3 film. Periodic modulation of intensity seen along q_z (vertical) is due to the X-ray standing wave that forms inside the thin film and is evidence to the good quality and uniformity of the bladed In_2O_3 films used in this study.

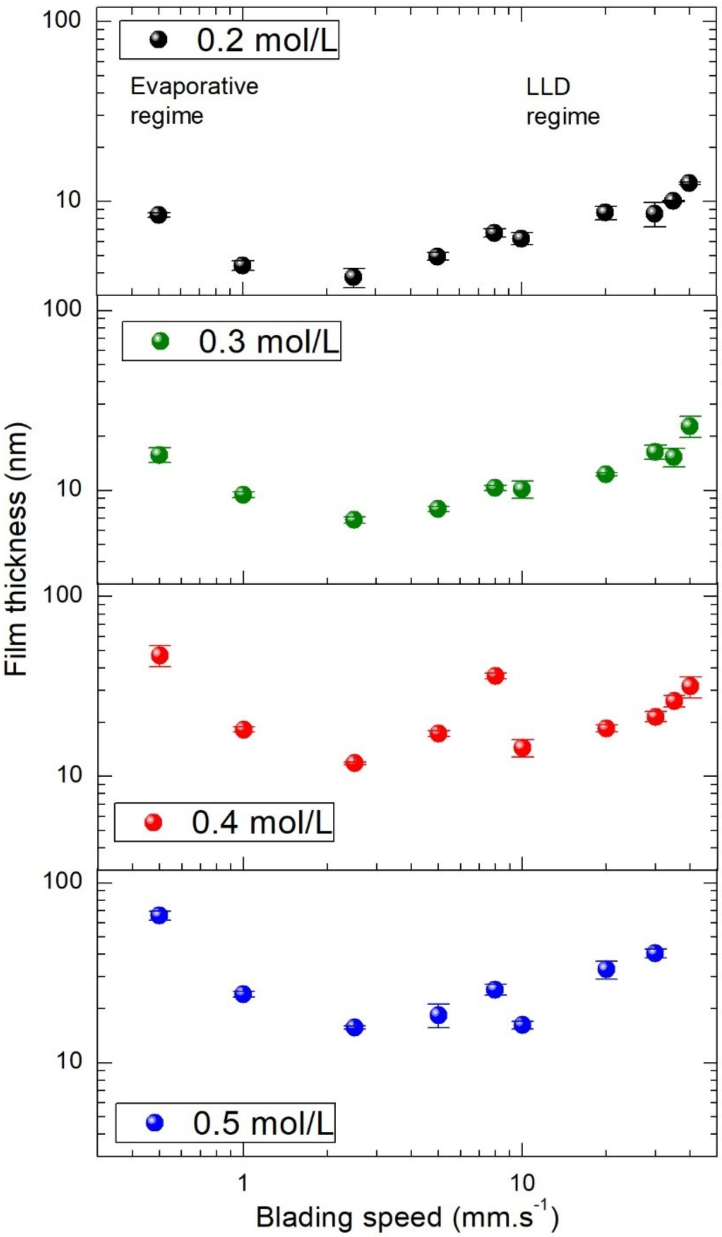

Figure S3. Thickness optimization of blade-coated sg-In_2O_3 films at 60 °C substrate temperature. Evaporative (lower speeds, negative slope) and Landau-Levich-Derjaguin (higher speeds, positive slope) coating regimes are clearly observed and suggest that the optimized films (5 mm s^{-1}) are coated in the Landau-Levich-Derjaguin regime. All uncertainties are ± one standard deviation of the mean.

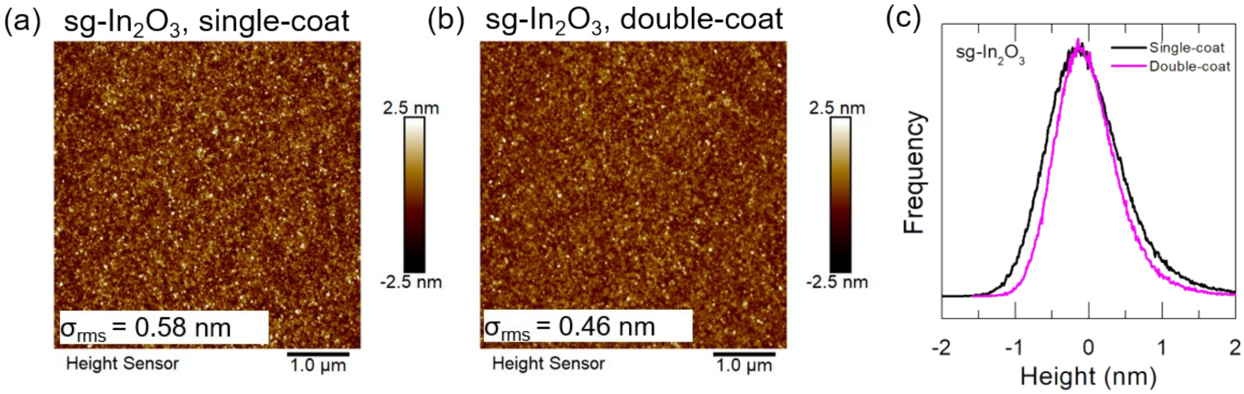

Figure S4. Atomic force microscopy (AFM) images showing the surface morphology of (a) single-coat (b) double-coat sg-In_2O_3 films, annealed at 325 °C. (c) Height histogram from the two images showing a slightly narrower surface roughness distribution for the double-coat film (pink).

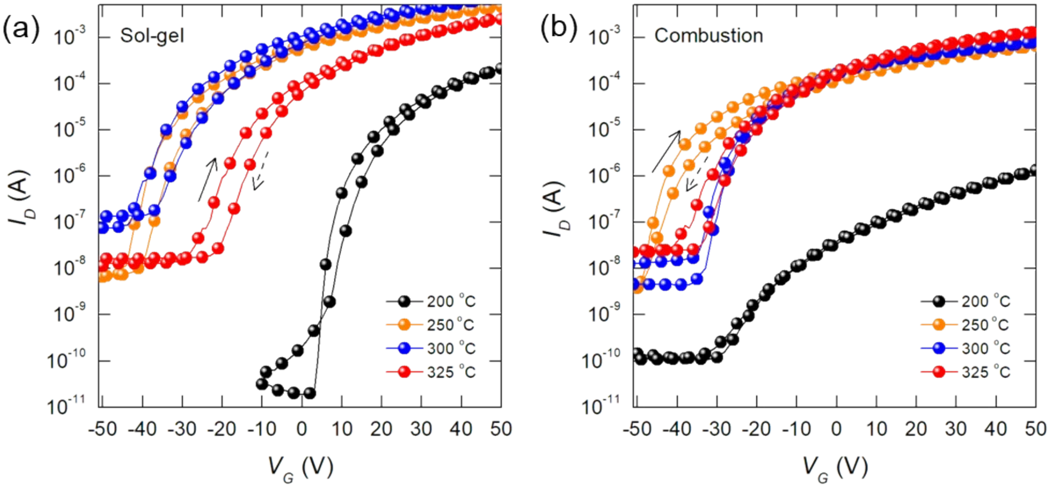

Figure S5. Forward and reverse sweeps of a few representative devices for (a) sg- and (b) c-In_2O_3 TFTs. Solid black arrow denotes forward sweep, while dashed black arrow denotes reverse sweep.

(a) Sol-gel

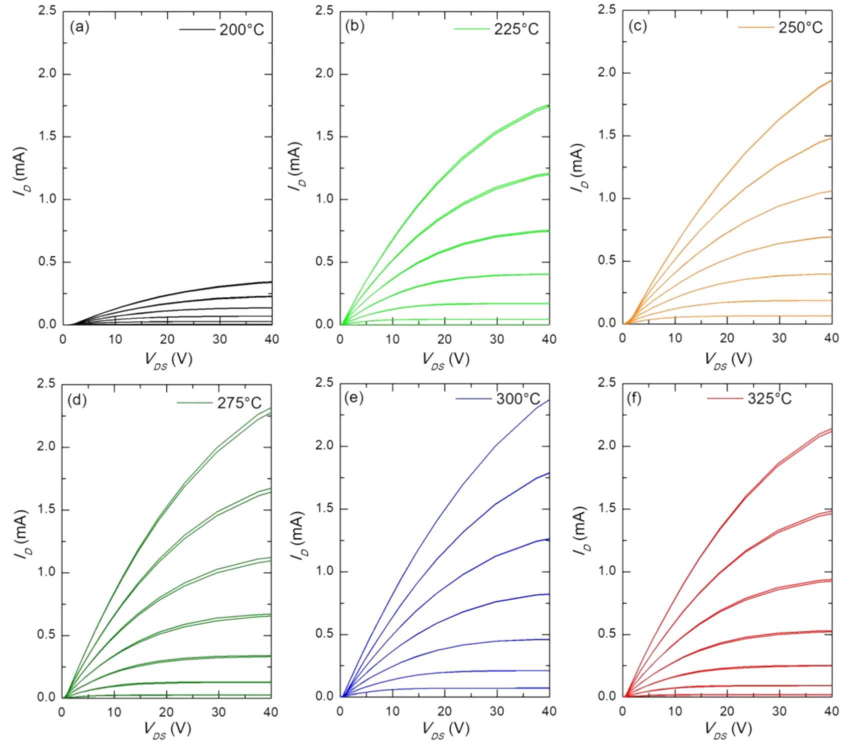

(b) Combustion

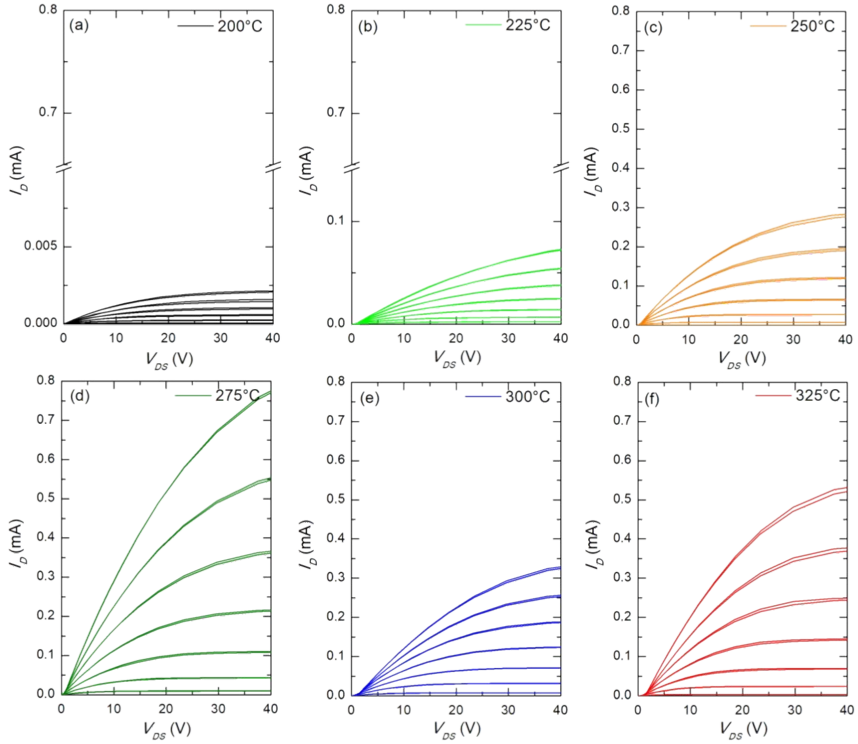

Figure S6. Representative output curves for (a). sg- and (b). c-In_2O_3 TFTs for all the annealing conditions considered in this study. V_{GS} = 0 V to 60 V, step = 10 V

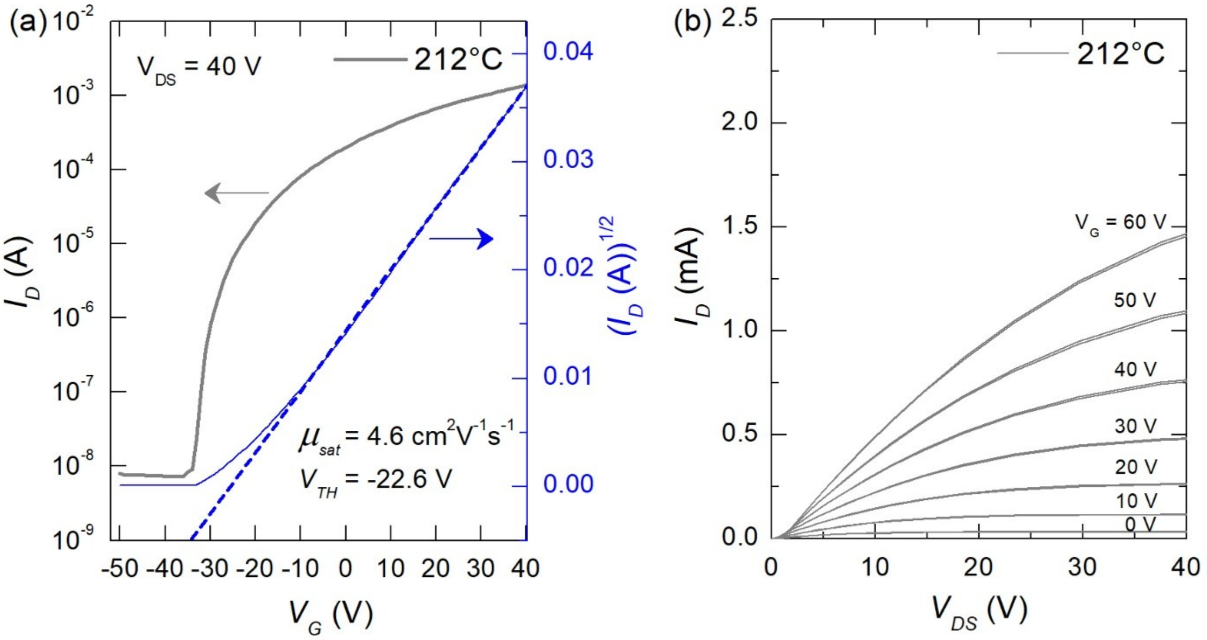

Figure S7. (a) Transfer, and (b) output curves for the best-performing 212 °C annealed sg-In_2O_3 TFT. Transfer curve was measured at a V_{DS} = 40 V, while output curves were measured in the range of V_{GS} = 0 V to 60 V with a step = 10 V.

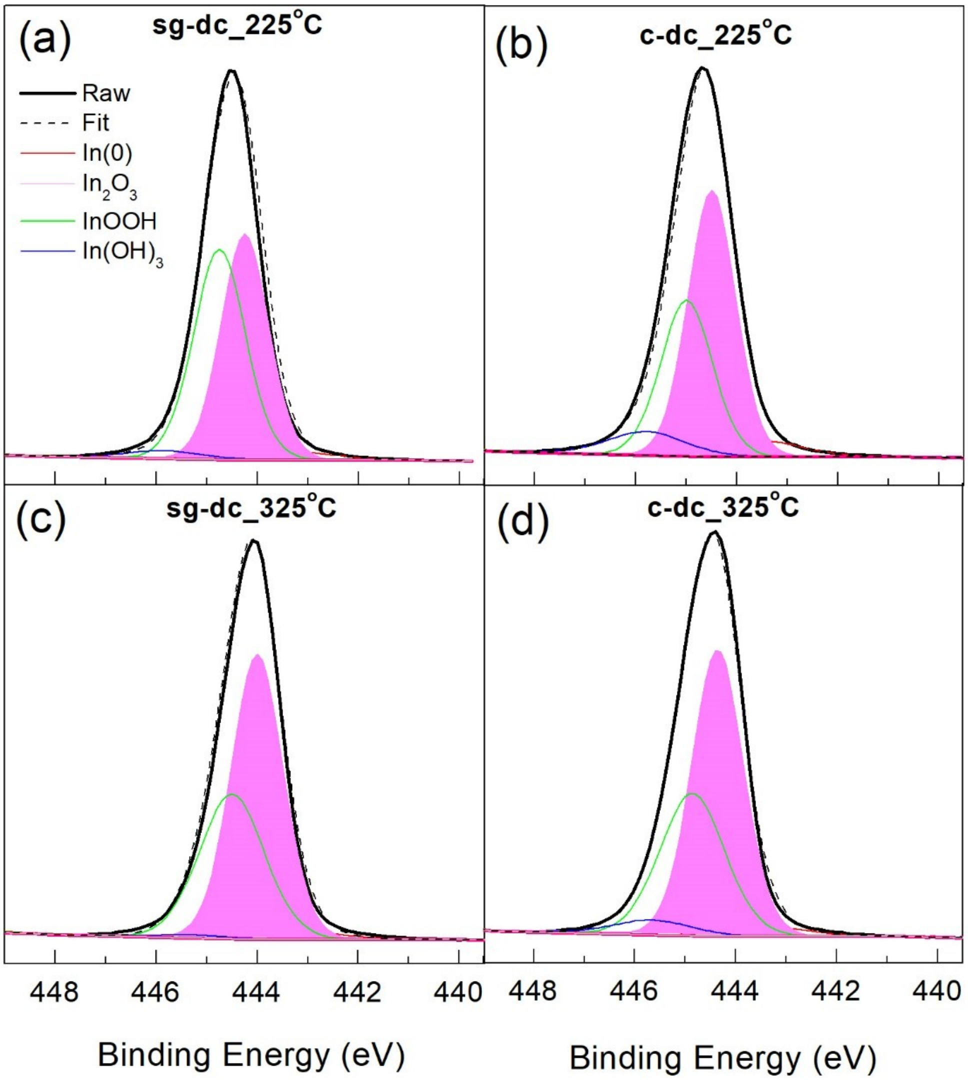

Figure S8. High-resolution X-ray photoelectron spectroscopy (XPS) spectra of the In $3d_{5/2}$ core level peaks. Pink component is the M-O-M lattice content. dc = double-coat (16 nm)

Table S1. Relative concentration of the various components of In $3d_{5/2}$ core level peak. dc = double-coat (16 nm)

Sample	M(0)	M-O-M	M-OH	M-OR
sg_dc_225	2.8	46.9	47.7	2.7
sg _dc_325	2.3	59.1	37.6	1.0
c _dc_225	5.5	52.9	33.9	7.7
c _dc_325	3.0	57.0	35.5	4.5

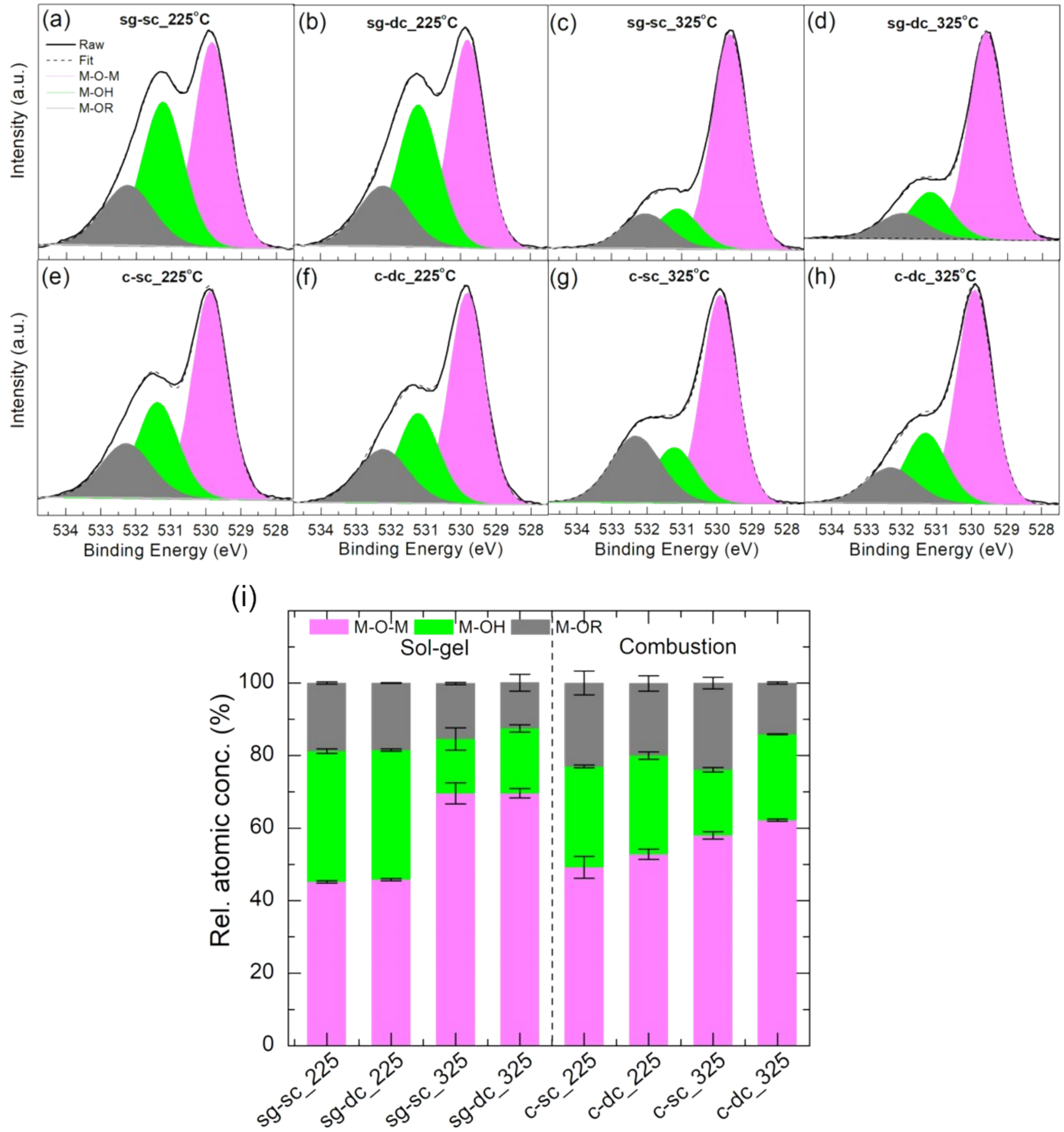

Figure S9. XPS data for O1s core level peak for the 8 nm single-coat (sc) films. For comparison, corresponding data on 16 nm double-coat (dc) is also shown. (i). Relative concentration of M-O-M, M-OH and M-OR components of the O1s peak. Error bars represent one standard deviation of the mean. sc = single-coat (8 nm), dc = double-coat (16 nm)

Table S2. M-O-M, M-OH and M-OR components (%) of the O1s core level for the different samples. sc = single-coat (8 nm), dc = double-coat (16 nm). ± represents one population standard deviation.

Sample	M-O-M	M-OH	M-OR
sg-sc_225	45.2 ± 0.3	36.0 ± 0.6	18.8 ± 0.3
sg-dc_225	45.8 ± 0.3	35.7 ± 0.3	18.5 ± 0.1
sg-sc_325	69.6 ± 2.9	15.0 ± 3.1	15.3 ± 0.3
sg-dc_325	69.6 ± 1.3	17.9 ± 1.0	12.6 ± 2.3
c-sc_225	49.2 ± 3.0	27.8 ± 0.4	23.0 ± 3.3
c-dc_225	52.8 ± 1.4	27.2 ± 1.0	19.9 ± 2.1
c-sc_325	58.0 ± 1.0	18.1 ± 0.6	23.9 ± 1.6
c-dc_325	62.2 ± 0.3	23.7 ± 0.1	14.1 ± 0.3

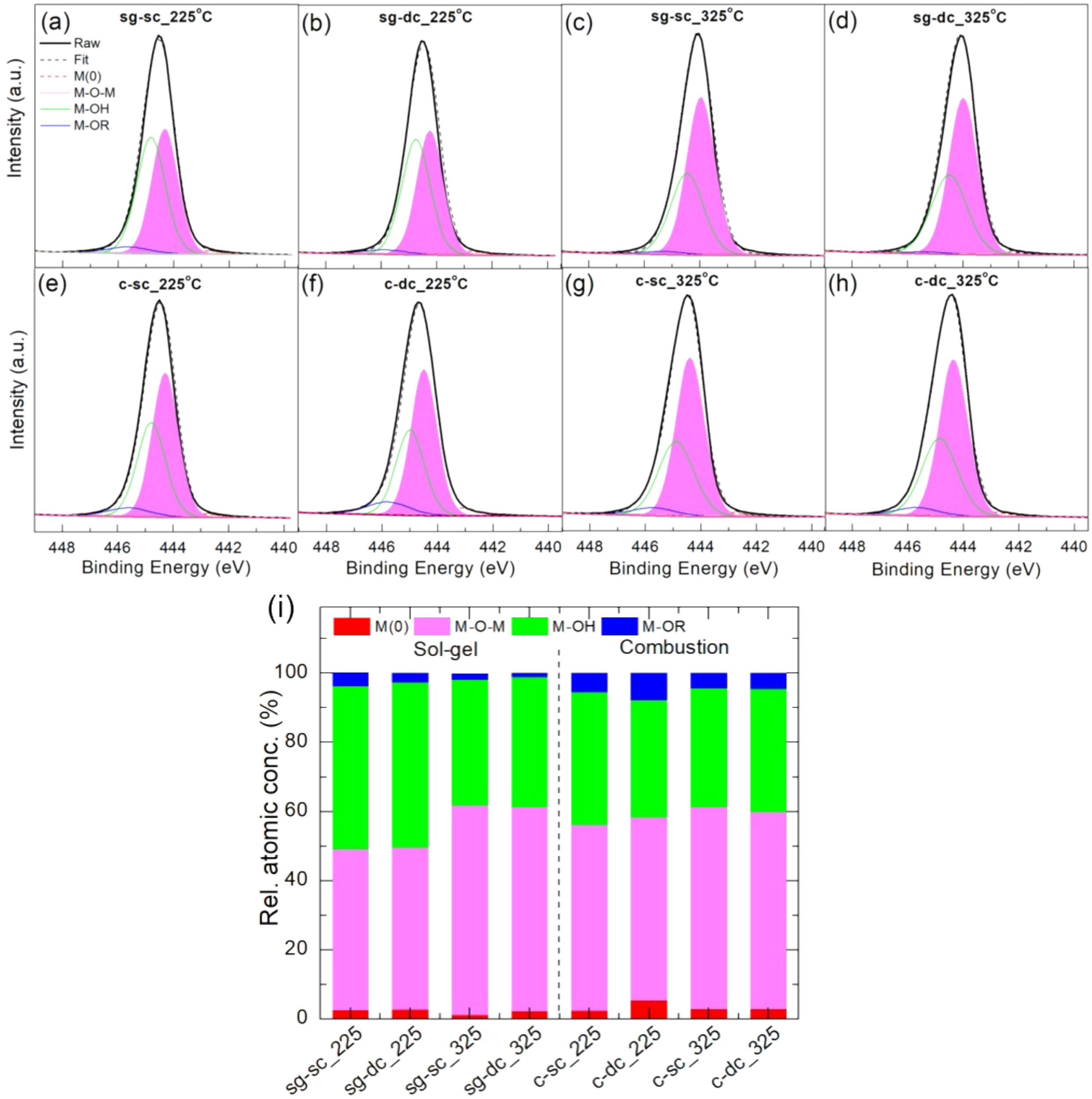

Figure S10. XPS data for In $3d_{5/2}$ core level peak for the 8 nm single-coat (sc) films. For comparison, corresponding data on 16 nm double-coat (dc) is also shown. (i). Relative concentration of the various components of In $3d_{5/2}$ peak. sc = single-coat (8 nm), dc = double-coat (16 nm)

Table S3. M(0), M-O-M, M-OH and M-OR components (%) of the In $3d_{5/2}$ core level for the different samples. sc = single-coat (8 nm), dc = double-coat (16 nm)

Sample	M(0)	M-O-M	M-OH	M-OR
sg-sc_225	2.7	46.4	47.2	3.9
sg-dc_225	2.8	46.9	47.7	2.7
sg-sc_325	1.3	60.5	36.4	1.7
sg-dc_325	2.3	59.1	37.6	1.0
c-sc_225	2.5	53.7	38.4	5.4
c-dc_225	5.5	52.9	33.9	7.7
c-sc_325	3.0	58.3	34.4	4.3
c-dc_325	3.0	57.0	35.5	4.5

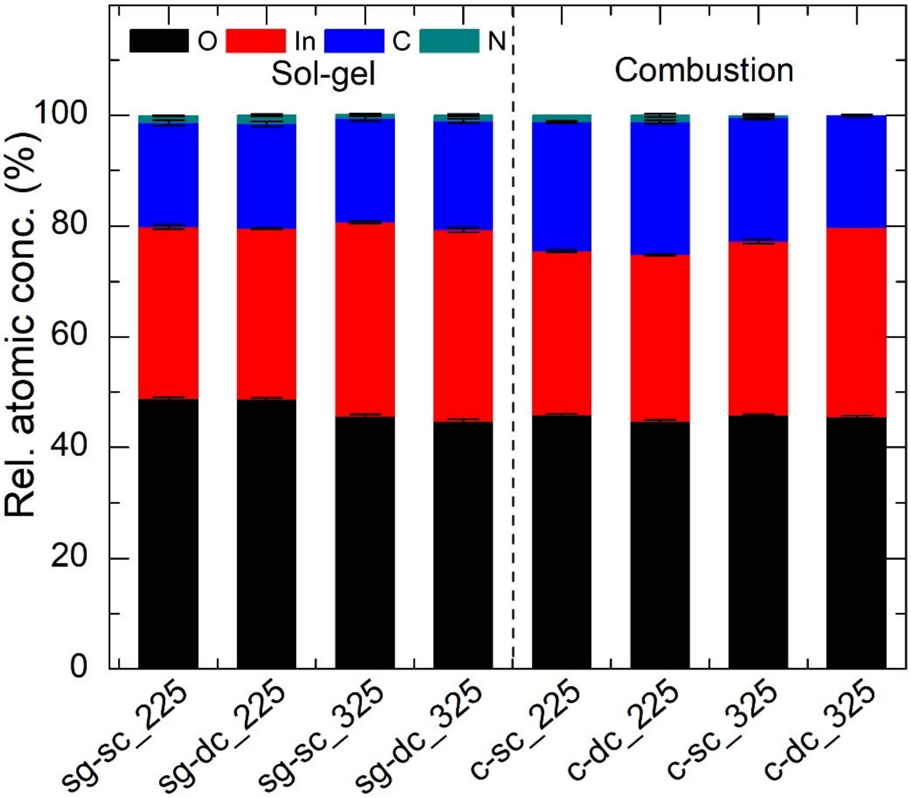

Figure S11. Relative atomic concentration of O, In, C and N for all the different In_2O_3 films considered in this study. sc = single-coat (8 nm), dc = double-coat (16 nm). Error bars represent one standard deviation of the mean.

Table S4. Relative atomic concentrations (%) for O, In, C and N for the different samples. Each value represents an average over 3 spots. sc = single-coat (8 nm), dc = double-coat (16 nm). ± represents one population standard deviation.

Sample	O	In	C	N
sg-sc_225	48.8 ± 0.3	31.0 ± 0.4	18.8 ± 0.5	1.3 ± 0.1
sg-dc_225	48.7 ± 0.3	30.8 ± 0.1	18.9 ± 0.5	1.6 ± 0.2
sg-sc_325	45.6 ± 0.4	35.1 ± 0.2	18.7 ± 0.4	0.7 ± 0.2
sg-dc_325	44.7 ± 0.4	34.6 ± 0.4	19.7 ± 0.4	1.0 ± 0.2
c-sc_225	45.9 ± 0.2	29.6 ± 0.2	23.3 ± 0.2	1.2 ± 0.0
c-dc_225	44.7 ± 0.3	30.1 ± 0.1	24.0 ± 0.3	1.2 ± 0.3
c-sc_325	45.8 ± 0.2	31.4 ± 0.4	22.4 ± 0.4	0.3 ± 0.3
c-dc_325	45.5 ± 0.3	34.2 ± 0.0	20.2 ± 0.2	0.0 ± 0.0